Chapter 3
Constraint and Dynamic Analysis of Compliant Mechanisms with a Flexible Multibody Modelling Approach

R.G.K.M. Aarts

Abstract The models used in the conceptual phase of the mechatronic design should not be too complicated, yet they should capture the dominant system behaviour. Firstly, the awareness and possibly the avoidance of an overconstrained condition is important. Secondly, the models should reveal the system's natural frequencies and mode shapes in a relevant frequency range. For the control system synthesis the low frequent behaviour up to the cross-over frequency needs to be known. Furthermore, the closed-loop system can be unstable due to parasitic modes at somewhat higher frequencies.

In this chapter the applicability of a multibody modelling approach based on non-linear finite elements is demonstrated for the mechatronic design of a compliant six DOF manipulator. A kinematic analysis is applied to investigate the exact constrained design of the system. From dynamic models the natural frequencies and mode shapes are predicted and a state-space model is derived that describes the system's input-output relations. The models have been verified with experimental identification and closed-loop motion experiments. The predicted lowest natural frequencies and closed-loop performance agree sufficiently well with the experimental data.

3.1 Introduction

In high precision equipment the use of compliant mechanisms is favourable as elastic joints offer the advantages of no friction and no backlash. For the conceptual design of such mechanisms there is no need for very detailed and complex models that are time-consuming to analyse. Nevertheless the models should capture the

R.G.K.M. Aarts (✉)
Faculty of Engineering Technology, University of Twente, P.O. Box 217, 7500 AE Enschede, The Netherlands
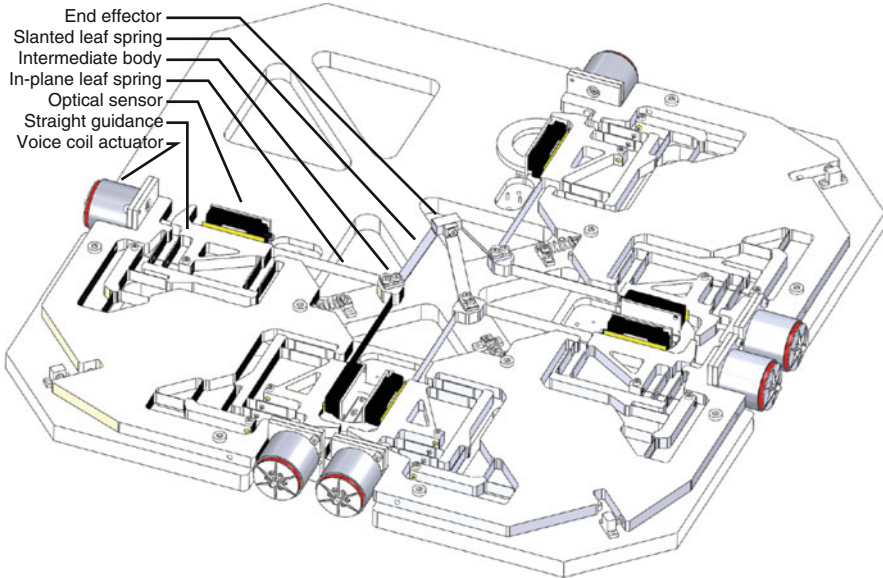e-mail: R.G.K.M.Aarts@utwente.nl

dominant system behaviour which must include relevant three-dimensional motion and geometric non-linearities, in particular when the system undergoes large deflections. More specifically, we distinguish two phases in the modelling approach of which a kinematic design is the first phase. Typical design considerations for this phase aim at detecting and where necessary avoiding overconstrained or underconstrained design in line with so-called Exact Constraint Design principles [1–3]. The dynamic system performance is considered in the second design phase. It involves the computation of the natural frequencies and the accompanying mode shapes, which are closely related to the required closed-loop bandwidth and stability of the mechatronic system [4, 5].

In [6–9] we discussed the use of the SPACAR software for these design phases. It offers a multibody approach based on non-linear finite elements. The sound inclusion of the non-linear effects at the element level [10] appears to be very advantageous. Only a rather small number of elastic beam elements is needed to model e.g. wire flexures and leaf springs accurately. In particular for the kinematic analysis to check the constraints only a single flexible beam element is used for each flexure. In a dynamic analysis the natural frequencies are computed and more beam elements may be used to obtain more accurate results at higher frequencies or for larger deflections. The non-linear model can be linearised in a number of configurations throughout the complete operational range of the mechanism to obtain a series of locally linearised models in terms of the independent degrees of freedom, e.g. state space models for control system design [11]. Numerically efficient models are obtained as the number of independent degrees of freedom is rather small. Consequently, the approach is particularly well suited during the early (mechatronic) design phase, where time consuming computations would severely hamper the design progress.

This chapter is an extension of a paper earlier presented [8]. The modelling approach will be applied for the analysis and MIMO control system synthesis of a parallel kinematic precision manipulator with six kinematic degrees of freedom (DOF) as is described in the next section. Numerical results are presented in Sect. 3.3 and are verified with experimental data. Finally conclusions are drawn.

3.2 Six DOF Manipulator

Figure 3.1 shows a six DOF hexapod-like flexure-based manipulator [12]. It is an scaled-up version of a micromanipulator originally designed to be manufactured with MEMS technology. It has to translate and rotate the end effector in all directions. It is difficult to accurately measure the motion of the small micromanipulator which is not more than a few mm in size. Sensors can be integrated much easier in the scaled-up manipulator which has a largest outer dimension of 540 mm. The large version should give insight in the dynamic behaviour of the micromanipulator and therefore the restrictions in the mechanical design resulting from the MEMS fabrication method have been preserved.

End effector ——
Slanted leaf spring ——
Intermediate body ——
In-plane leaf spring ——
Optical sensor ——
Straight guidance ——
Voice coil actuator ——

Fig. 3.1 Six DOF hexapod-like manipulator with flexible joints [12]

In the scaled-up manipulator six voice coil actuators (VCMs) are applied to drive the position and orientation of the end effector. In the MEMS design it is essential that each actuator is constrained to a purely translational motion. In the scaled-up version this motion is also enforced by straight guidances that assure that the motion of each VCM is exactly in one in-plane direction. Each VCM is equipped with a contact-free optical incremental encoder to measure the actuator displacement for colocated feedback control. The motions of a pair of VCMs are transferred via in-plane leaf springs to an intermediate body, such that this body can move in the in-plane directions. In total three of these intermediate bodies support three slanted leaf springs that are connected to the end effector. In this way the three times two in-plane actuated translations of the intermediate bodies enable translations and rotations of the end effector in all six DOF. E.g. the horizontal translations of the end effector are realised with identical motions of all three intermediate bodies. To accomplish a vertical translation of the end effector, the three intermediate bodies move radially towards the centre of the set-up. These motions and the rotations are outlined in more detail by Brouwer et al. [12]. In general, the relations between the linear VCM displacements and the position and orientation of the end effector are highly non-linear. These relations can be measured with a sensor system that is mounted on the end effector. This sensor system (not shown in Fig. 3.1) includes an optical sensor to measure the displacement in one long-stroke direction, while the parasitic displacements in the perpendicular directions and the rotations are measured with capacitive sensors.
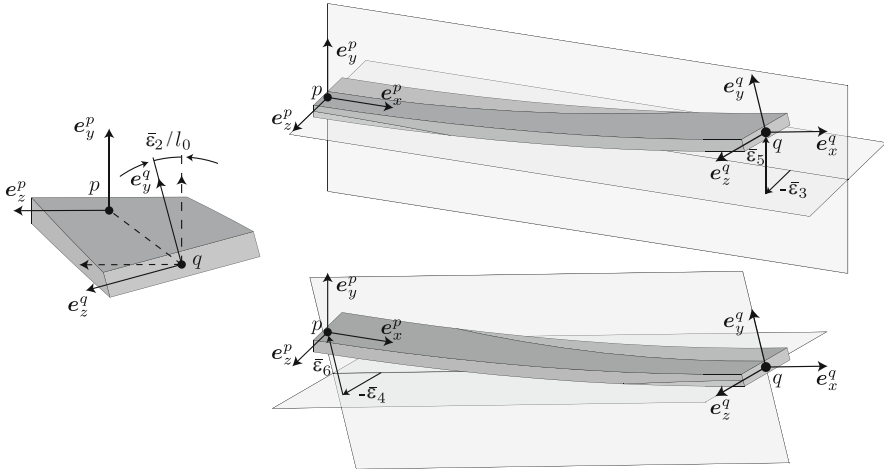
Fig. 3.2 Deformations ε_2–ε_6 of the spatial beam element (Reprinted from [14])

3.3 Numerical Modelling

A numerical model of the manipulator needs to account for the flexures in the system. More specifically each straight guidance consists of leaf springs and a wire spring. The end effector is mounted on the three slanted leaf springs. In the modelling approach implemented in SPACAR flexible beam elements are used for all flexures. This beam element will be outlined first before the kinematic and dynamic analyses are presented.

3.3.1 Spatial Flexible Beam Element

The location of the beam element is described by the positions of the end nodes p and q, as well as their orientations. Essential is the definition of physically meaningful deformation modes of the element that are invariant for rigid body motions of the element. As there are 12 independent nodal coordinates and six rigid body degrees of freedom, six independent deformation modes can be defined. For the spatial flexible beam one deformation mode coordinate ε_1 is taken to describe the elongation, ε_2 for torsion and four modes ε_{3-6} for the bending deformations of the element [10, 13]. Figure 3.2 illustrates five of these deformation modes. The deformation mode coordinates are defined in such a way that geometrically non-linear effects due to interaction between deformation modes are included. Consequently, accurate models can be obtained with a relatively small numbers of elements even for the case when large deflections are considered [10, 13]. Each of the deformation mode coordinates can be defined to be constrained or released.

If a deformation mode coordinate is released, i.e. not constrained, constitutive equations have to be specified for the stress resultants, which are dual to the deformations. These constitutive equations may express simply linear elastic behaviour based on the element stiffness properties.

3.3.2 Kinematic Model and Exact Constrained Design

Numerical models of the system can be made with a varying level of complexity. With a *kinematic* SPACAR model it can be verified that the manipulator satisfies exact constraint design. In this model each wire flexure and leaf spring is modelled with a single flexible beam element. All deformation modes with a high stiffness are considered to be rigid, i.e. having constrained deformation mode coordinates. The deformation modes with low stiffnesses are allowed to deform. Then it appears that a Jacobian matrix can be assembled which must be square and full rank in order to satisfy exact constraint design: otherwise the system is underconstrained or overconstrained [7, 9].

The straight guidances of the manipulator, Fig. 3.3, are overconstrained by design to increase the stiffness in the out-of-plane direction. This is confirmed in the kinematic analysis and these parts are manufactured accurately to minimise the internal stresses [12]. A six DOF kinematic model confirms the exact constraint design of the end effector motion, Fig. 3.4.

Note that for this kinematic analysis the masses and stiffnesses do not play a role. These are of course relevant in the dynamic analysis to be discussed next.

3.3.3 Dynamic Model and Natural Frequencies with Mode Shapes

Natural frequencies and mode shapes are obtained from *dynamic* models. The simplest dynamic model is derived from the kinematic model outlined above in which mass and stiffness properties are added. In the applied modelling approach the non-linear equations of motion can be linearised in any valid configuration of the system. From the mass and stiffness matrices the (configuration dependent) natural frequencies and mode shapes are computed. A state space model is derived after defining the system's inputs, the VCM forces, and outputs, the colocated sensor positions. As the simplest dynamic model has six DOF, only the six lowest natural frequencies of the manipulator can be obtained from this model and a twelfth order state space model is found.

For control system synthesis also higher natural frequencies and their mode shapes must be known [4]. These so-called parasitic modes involve deformations in the directions of the larger stiffnesses. In the dynamic model they can be accounted for by releasing deformation mode coordinates associated with deformations in
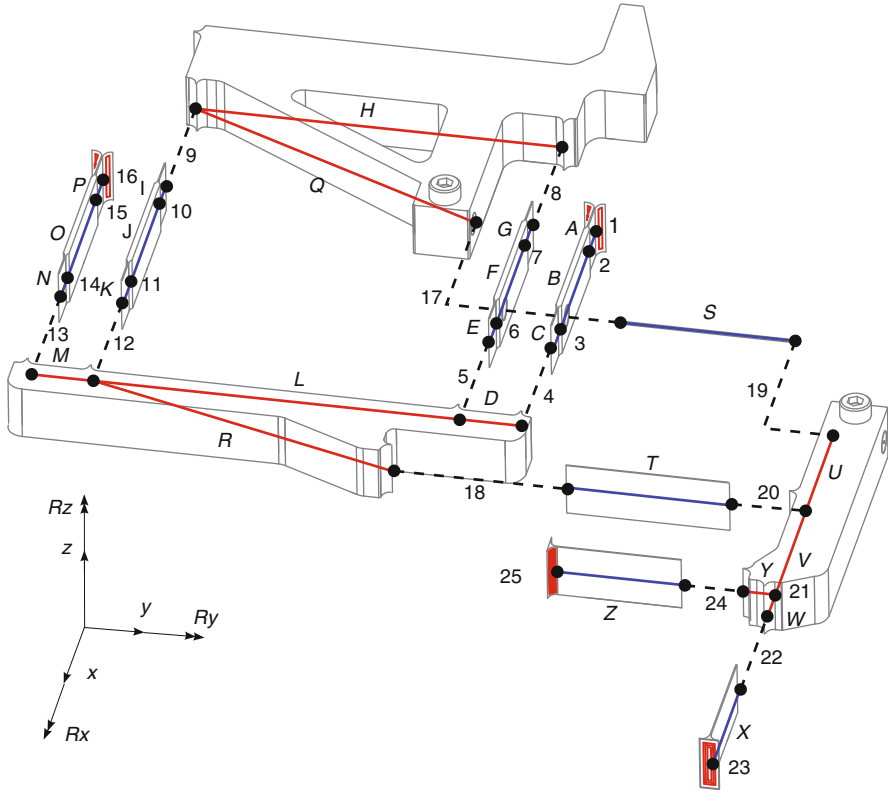
Fig. 3.3 Schematic model of each straight guidance. The lines in the solid parts represent rigid elements. The lines in the flexures ABC, EFG, IJK, NOP, S, T, X and Z are flexible beam elements. The dashed lines are connections between elements that are apart for a clearer view. In the points *1*, *16*, *23* and *25* the guidance is fixed to the world. The motion of body H is guided. Lever U assures that the stroke of the intermediate body L is half of the stroke of body H (From [15])

these directions. In the previous six DOF model these deformations were prescribed zero and now these released deformation mode coordinates give rise to additional degrees of freedom. Furthermore, the system should be evaluated in configurations throughout the manipulator's workspace. The six deformation modes of the flexible beam element offer only an accurate approximation for a limited set of element deformations. If more complex deformations are expected, the approximation can be improved by increasing the number of elements in each flexure. Obviously, both improvements of the dynamic model result in an increased number of DOF.

For the considered manipulator a model has been made in which three or four beam elements are used for each wire flexure of leaf spring. This model has 870 DOF which result in many natural frequencies that are far outside the frequency range of interest. To reduce the number of DOF the model is first simplified by reducing the number of beam elements that is used for the flexures. If the lower natural frequencies of the reduced order model are identical or close to the natural
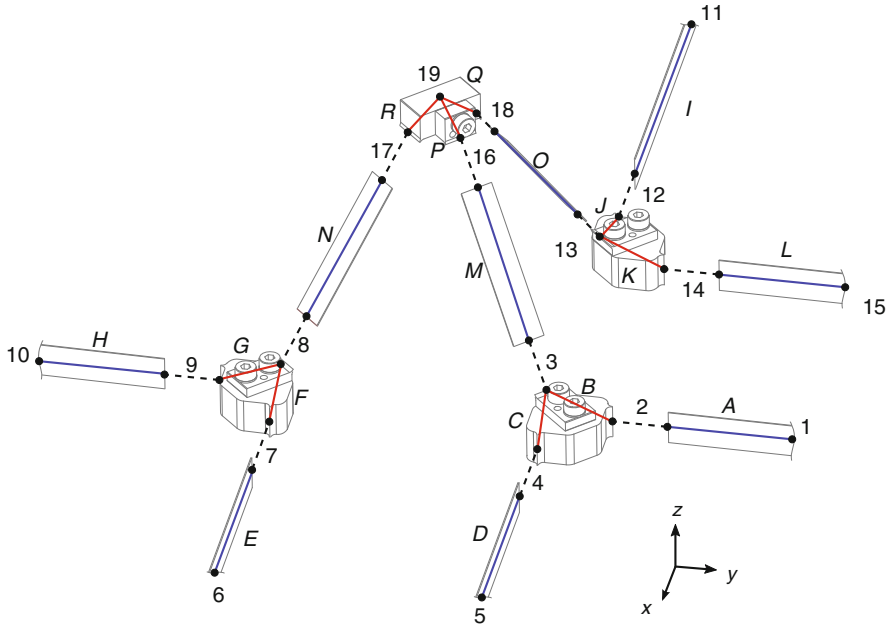
Fig. 3.4 Schematic model of the end effector. The lines in the solid intermediate bodies and end effector represent rigid elements. The lines in the flexures A, D, E, H, I, L, M, N and O are flexible beam elements. The dashed lines are connections between elements that are apart for a clearer view. In the points *1*, *5*, *6*, *10*, *11* and *15* purely translational motions are prescribed which cause in-plane motion of the intermediate bodies *C*, *G* and *K*. As a result, the out-of-plane leaf springs *M*, *N* and *O* move the end effector (points *16–19*) in all translational and rotational degrees of freedom (From [15])

frequencies of the 870-DOF model in this range, the simplification is accepted. In this way the number of DOF could be reduced to 420. A further simplification is possible by constraining deformations. The longitudinal stiffness of the flexures is rather high and it appears that a model with all elongations ε_1 prescribed zero results in 315 DOF without loss of accuracy. Similarly also part of the bending deformation modes with a high stiffness can be considered rigid and finally a 237-DOF model is obtained. Table 3.1 lists the numerical values of the ten lowest natural frequencies of both the extended 870-DOF and the reduced 237-DOF models. As can be seen in the table the lowest six natural frequencies of the reduced model are almost identical to the natural frequencies of the large model. For the higher natural frequencies somewhat larger differences are found. For the control system synthesis, in particular the seventh natural frequency is relevant which differs by about 6%. In Fig. 3.5 these natural frequencies can be recognised as the peaks in the graph of the system's singular values or principal gains as functions of the frequency. In this analysis the VCM forces are the system's inputs and the colocated sensors are the outputs. The lowest natural frequencies are damped due to the actuator's back-EMF.

Table 3.1 First ten natural frequencies (in rad/s) of the large and reduced models as well as the experimentally identified natural frequencies. Note that the experimentally observed 7th and 8th natural frequency are not present in the models

Mode	870-DOF	237-DOF	Mode	Exp.
1	59.3	59.3	1	55.3
2	59.9	59.9	2	56.0
3	84.3	84.5	3	79.6
4	86.8	86.8	4	83.0
5	122.0	122.2	5	116.1
6	124.6	125.1	6	120.2
			7	225
			8	285
7	658	697	9	565
8	844	917		
9	908	1001	10	1050
10	1074	1303		
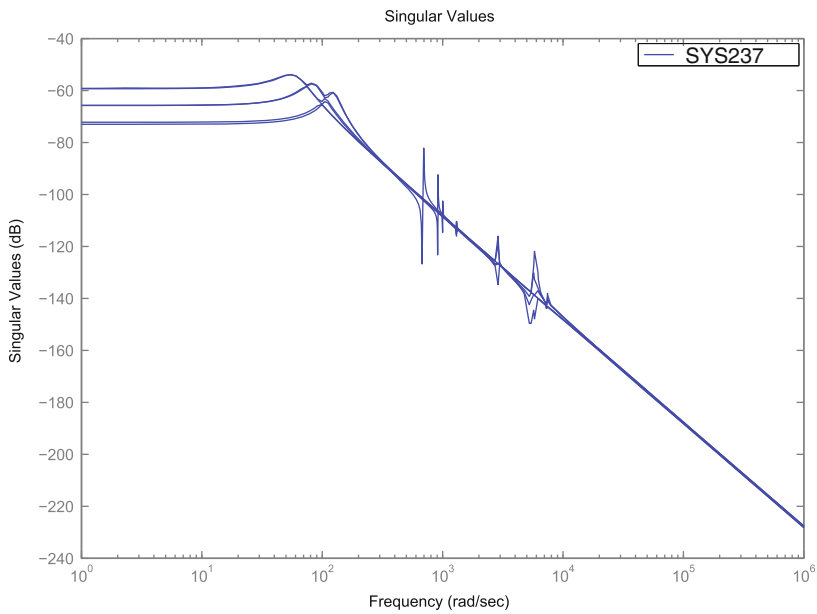
Fig. 3.5 Singular values of the transfer matrix of the 237-DOF SPACAR-model near the equilibrium configuration (From [15])

The linearised models of the mechanical system are well-suited for control system synthesis. The following steps are taken. At first the cross-over frequency of the feedback controller is determined from performance requirements. Assuming this cross-over frequency will be well below the unwanted higher natural frequencies, the closed-loop performance can be evaluated from the controller combined with the low frequent behaviour of the mechanical system [4], i.e. the six lowest natural frequencies. For this purpose a linearised six DOF model that accounts for the lowest six natural frequencies in Table 3.1 is well-suited. As an example we consider a PID-like feedback controller that should track a third order motion profile during 1 s with an error of less than 0.1% of the amplitude. This can be accomplished with a cross-over frequency of about 300 rad/s. Secondly, the closed-loop performance can be improved with feedforward control. A feedforward control input can be computed by applying a stable inverse approximation of a low frequent model of the mechanical system to the desired motion profile.

Finally the robust stability of this closed-loop system can be evaluated. In particular the first parasitic natural frequency may violate stability requirements in an $\mathcal{H}_\infty$ controller design strategy [4]. Obviously for this purpose a model of the mechanical system like the 237-DOF model is needed that is sufficiently accurate above the cross-over frequency. This model can also be used in closed-loop simulations to validate the controller design.

3.4   Experimental Results

An experimental set-up with the manipulator of Fig. 3.1 has been realised. As outlined in Sect. 3.2 it is actuated with six VCMs. Colocated sensors measure the actuator displacements. MIMO system identification has been carried out with a black-box multivariable output error subspace (MOESP) model identification method [15–17]. A 21st order model is found that identifies the lowest natural frequencies as well as the first parasitic modes. These natural frequencies are included in Table 3.1 and are combined with the 237-DOF model in Fig. 3.6. It appears that the six lowest natural frequencies agree quite well between the numerical model and experimental data. Also the natural frequency of the first parasitic mode agrees reasonably well. However, two additional natural frequencies are found in the identification that are not included in the models. Probably these modes arise from suspension modes of the frame that are not accounted for in the numerical models. In Fig. 3.6 these modes are visible, but their amplitudes are rather small. Overall it is concluded that the numerical models provide an adequate prediction of the experimental results.

The designed feedback and feedforward controller has been tested for a motion of the end effector of 6 mm displacements in the horizontal x, y-plane. Figure 3.7 shows the tracking error of the actuator displacements during this motion. It appears
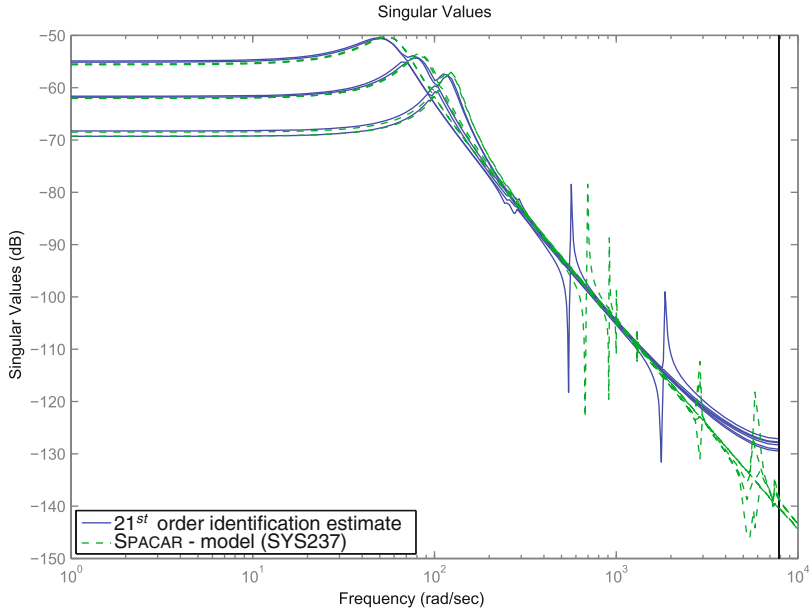
Fig. 3.6 Singular values of the transfer matrix of the 21st order identification estimate and the SPACAR-model near the equilibrium configuration (From [15])
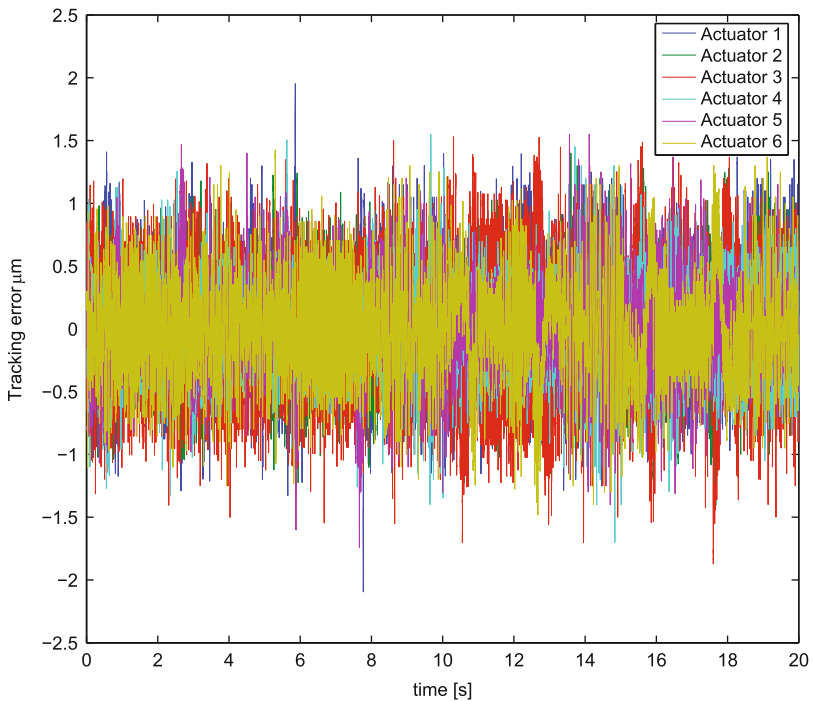
Fig. 3.7 Measured tracking error of the actuator displacements during a 6 mm displacement of the end effector in the *x*, *y* -plane (From [15])
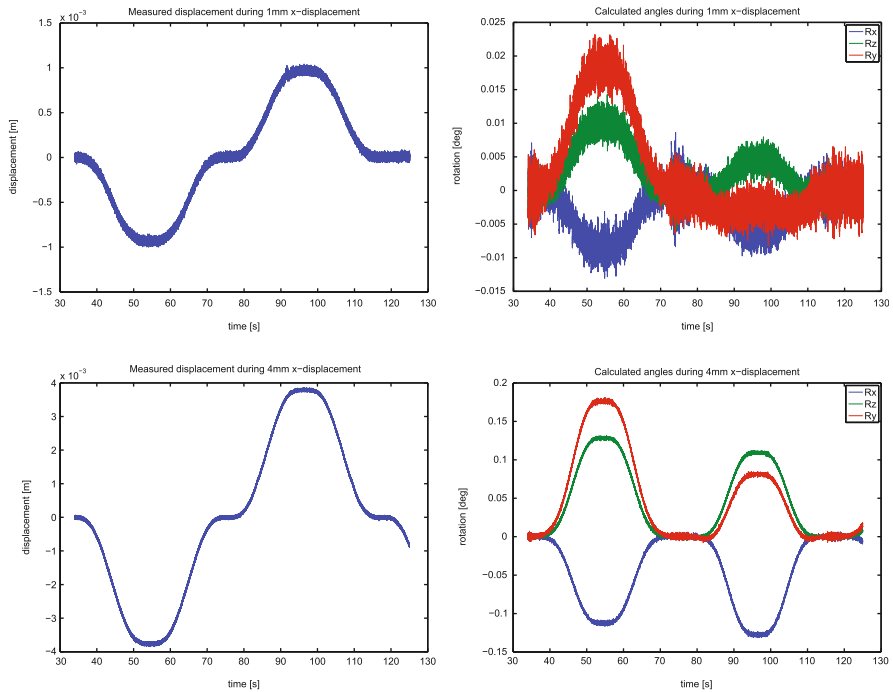
Fig. 3.8 Measurements of the end effector motion during 1 mm (*top*) and 4 mm (*bottom*) *x*-displacements of the end effector. The left graphs show the long stroke motion in the *x* direction; the right graphs show all three rotations of the end effector for both displacements (From [15])

that they remain below the desired 0.1% although the signal is quite noisy. This is to a large extend caused by a 50 Hz disturbance from the mains.

Finally, the motion of the end effector has been analysed with the sensor mounted on the end effector. This sensor can measure a long stroke in one direction and small deviations in the other directions as well as rotations. The *x* axis of the coordinate system is aligned with the direction of the long stroke. The linearised manipulator model has been used to compute the actuator displacements needed for linear displacements of the end effector in the *x* direction of 1 mm and 4 mm, respectively. Figure 3.8 shows the actually measured motion of end effector. It is found that the real displacement matches reasonably with the intended motion, but it is somewhat smaller than expected. Furthermore, unwanted rotations are observed. To some extend both effects can be caused by a small misalignment between the coordinate systems of the manipulator and the sensor. However, it is also noted that the deviations increase more than linearly when the amplitude of the end effector displacement is increased. This could be caused by the non-linear behaviour of the manipulator which is not yet included in the model currently used to compute the needed actuator displacements.

3.5   Conclusions

The design of a mechatronic system of the six DOF compliant manipulator in
Fig. 3.1 demonstrates the proposed modelling approach for this purpose. The
formulation is based on a nonlinear finite element description for flexible multibody
systems. The flexible beam elements account for geometric nonlinear effects such
as geometric stiffening and interaction between deformation modes. Flexible joints
like wire flexures and leaf springs can be modelled adequately using only a few
number of flexible beam elements. In this way, a rather low dimensional system
description can be obtained which includes the non-linear behaviour that occurs at
large deflections.

In a kinematic analysis only a single flexible beam element is used for each wire
and sheet flexure and the exact constrained design of the system is examined. In
particular overconstrained conditions are detected and if necessary the design can
be modified to avoid these overconstraints. For the dynamic analysis a maximum of
four flexible beam elements is used for each flexure. The number of DOF is reduced
by prescribing deformations with high stiffness and in rigid parts to be zero. In any
configuration of the manipulator the natural frequencies and mode shapes can be
computed. Furthermore, an input-output state space model can be derived to design
and evaluate the control system. The modelling approach is well suited for
mechatronic design, i.e. the mechanical design as well as control system synthesis.

References

1. Blanding DL (1999) Exact constraint: machine design using kinematic principles. ASME
   Press, New York
2. Hale LC (1999) Principles and techniques for designing precision machines. Ph.D. thesis,
   University of California, Livermore
3. Soemers HMJR (2010) Design principles for precision mechanisms. T-point print, Enschede
4. van Dijk J, Aarts RGKM, Jonker JB (2012) Analytical one parameter method for PID motion
   controller settings. In: IFAC conference on advances in PID control – PID'12, Brescia, 28–30
   Mar 2012
5. Xu JX (2008) New lead compensator designs for control education and engineering. In:
   Proceedings of 27th Chinese control conference, 16–18 July 2008
6. Aarts RGKM, van Dijk J, Jonker JB (2009). Efficient analyses for the mechatronic design of
   mechanisms with flexible joints undergoing large deformations. In: ECCOMAS thematic
   conference multibody dynamics 2009, Warsaw University of Technology, Warsaw,
   June 29–July 2

7. Aarts RGKM, van Dijk J, Jonker JB (2010) Flexible multibody modelling for the mechatronic design of compliant mechanisms. In: The 1st joint international conference on multibody system dynamics, Lappeenranta, 25–27 May 2010
8. Aarts RGKM, van Dijk J, Brouwer DM, Jonker JB (2011) Application of flexible multibody modelling for control synthesis in mechatronics. In: Multibody dynamics 2011, ECCOMAS thematic conference, Brussels, 4–7 July 2011
9. Aarts RGKM, Boer SE, Meijaard JP, Brouwer DM, Jonker JB (2011) Analyzing overconstrained design of compliant mechanisms. In: Proceedings of ASME 2011 international design engineering technical conference & computers and information in engineering conference – IDETC/CIE 2011, Washington, DC, 28–31 Aug 2011
10. Jonker JB, Meijaard JP (2009) Definition of deformation parameters for the beam element and their use in flexible multibody system analysis. In: ECCOMAS thematic conference multibody dynamics 2009, Warsaw University of Technology, Warsaw, June 29–July 2
11. Jonker JB, Aarts RGKM, van Dijk J (2009) A linearized input-output representation of flexible multibody systems for control synthesis. Multibody Syst Dyn 21(2):99–122
12. Brouwer DM, de Jong BR, Soemers HMJR (2010) Design and modeling of a six DOF's MEMS-based precision manipulator. Precis Eng 34(2):307–319
13. Meijaard JP, Brouwer DM, Jonker JB (2010) Analytical and experimental investigation of a parallel leaf spring guidance. Multibody Syst Dyn 23(1):77–97
14. Boer SE, Aarts RGKM, Brouwer DM, Jonker JB (2010) Multibody modelling and optimization of a curved hinge flexure. In: The 1st joint international conference on multibody system dynamics, Lappeenranta, 25–27 May 2010
15. Spijksma SA (2010) Analysis and MIMO control of a 6 DOFs parallel kinematic precision manipulator. M.Sc. thesis, Report number Wa-1293, University of Twente, Enschede
16. Nijsse G (2006) A subspace based approach to the design, implementation and validation of algorithms for active vibration isolation control. PhD thesis, University of Twente, Enschede
17. van Overschee P, de Moor B (1994) N4SID: subspace algorithms for the identification of combined deterministic-stochastic systems. Automatica 30(1):75–93